Microviscosity Measurements of Phospholipid Bilayers Using Fluorescent Dyes That Undergo Torsional Relaxation†

Chun En Kung and Juta K. Reed*

J. Tuzo Wilson Research Laboratories, Department of Chemistry, University of Toronto, Mississauga, Ontario, L5L 1C6 Canada

Received April 7, 1986

ABSTRACT: Fluorescent dyes that undergo solvent-dependent intramolecular rotational relaxation are potentially of great value in the study of the viscosity of surfactant micelles, natural membranes, and artificial phospholipid bilayers. One such dye, 9-(dicyanovinyl)julolidine (DCVJ), is an example of a series of previously well-characterized charge-transfer malononitrile derivatives whose fluorescence quantum yield is solvent viscosity dependent [Loutfy, R. O., & Arnold, B. A. (1982) *J. Phys. Chem. 86*, 4205-4211]. This dye has been used to estimate the effective microviscosity of sodium dodecyl sulfate (SDS) micelles and of small unilamellar dipalmitoylphosphatidylcholine (DPPC) vesicles. Estimates of effective microviscosity were made from quantum yield measurements with the free volume concept developed for medium- to high-viscosity solvents ($\eta \geq 2$ cP). Effective microviscosities in DPPC vesicles range from 70 to 120 cP between 60 and 10 °C with a transition observed at 34 °C. Activation energies for solvent or hydrocarbon chain mobility [$\Delta E(\eta)$] were 6.9 and 14.7 kJ/mol above and below this transition, respectively. These values closely parallel the estimated activation energies for the torsional relaxation of the dye [$\Delta E(k_{or})$] and are remarkably similar to the activation energies associated with the fast trans-gauche isomerizations in fatty acyl chains reported from NMR measurements. These results are consistent with the view that the rotational dynamics of the fluorescent dye report on the reorientational relaxation of the hydrocarbon chains within the bilayer. From the measured fluorescent peak maximum, the dye is believed to be located in an environment with a dielectric constant of 17.9, certainly well within the interior of the hydrocarbon core. At 25 °C in SDS micelles, the dye reports a more polar, surface interface environment ($\epsilon = 41.6$) with a much lower effective microviscosity (6.9 cP).

The dynamic properties of the phospholipid matrix are known to profoundly affect many of the physiological functions associated with biological membranes. Changes in such physical properties of bilayers as thermal phase transitions, lateral phase separations, local dielectric properties, and rotational diffusion are believed to modulate the biological activity of a wide range of membrane-associated receptors, transport proteins, and enzymes, among others. Fluorescence spectroscopy is currently one of the most widely used techniques available to study these properties. Environmentally sensitive fluorophores of varying structural complexity have been shown to report on most, if not all, of these dynamic phenomena, both in natural as well as in model membrane and micellar systems (Lakowicz, 1983; Schlessinger & Elson, 1982; Yguerabide & Foster, 1982).

One major focus of the work has been aimed at the determination of the apparent or effective membrane "microviscosity" (Grieser et al., 1985; Schlessinger & Elson, 1982). Unfortunately, many membrane microviscosity values reported for different fluorophores are often dependent upon the molecular characteristics of the probe (Viriot et al., 1983). Generally, when the fluorophore requires a large volume for motion, whether it be for excited-state formation or nonradiative deexcitation, a wide range of microviscosities is obtained. The possibility that the large probe may cause membrane bilayer distortion has been suggested (Grieser et al., 1985).

In addition to reporting bilayer microviscosities and phase behavior, fluorescent probes often provide information on the local dielectric properties of their environment (Law, 1981; Thomas, 1980). Usually the fluorescence emission characteristics can be related to the dielectric constant of a solvent in a standard solvent scale. Only a few fluorophores are capable of providing useful information on both membrane microviscosity and local dielectric properties.

The most widely used luminescence techniques for studying bilayer microviscosity are steady-state or dynamic depolarization and diffusion-dependent inter- and intramolecular excimer formation (Thomas, 1980; Yguerabide & Foster, 1982). However, these techniques have limitations. For example, the concentrations required for effective intermolecular pyrene excimer formation in lipid bilayer often lead to probe aggregation because of nonuniform probe distribution (Thomas, 1980). Microviscosities obtained from intramolecular excimer formation are more dependent on the structural characteristics of the probe rather than on the environment itself (Viriot et al., 1983). The calculation of microviscosities from steady-state depolarization requires the assumption of isotropic probe motion in the bilayer, an assumption that may not be valid for most nonpolar fluorophores (Schlessinger & Elson, 1982). In fact, the range of microviscosity values reported for dipalmitoylphosphatidylcholine (DPPC)[1] vesicles for example varies from 30 to 1000 cP.

Recently, Loutfy and his colleagues have shown that twisted intramolecular charge-transfer molecules can be useful in the

† This research was supported by Natural Sciences and Engineering Research Council of Canada Grant A0498.

* Author to whom correspondence should be addressed.

[1] Abbreviations: DCVJ, 9-(dicyanovinyl)julolidine; DPPC, dipalmitoylphosphatidylcholine; SDS, sodium dodecyl sulfate; DMPC, dimyristoylphosphatidylcholine; EPC, egg phosphatidylcholine; DPH, 1,6-diphenyl-1,3,5-hexatriene.

0006-2960/86/0425-6114$01.50/0

study of polymeric reactions where large changes in microviscosities occur (Law & Loutfy, 1981, 1983; Loutfy, 1981). One such group of molecules, [*p*-(dialkylamino)-benzylidene)]malononitriles has been extensively studied as possible environmental probes (Law, 1980, 1981). The excited single state, S_1 of these molecules consists of a π,π^* intramolecular charge-transfer state. The deactivation of this state is dominated by a rapid ($k_{nr} \approx 10^{11}$ s^{-1}) nonradiative internal conversion attributed to torsional relaxation about the donor–acceptor bond. Restrictions on this molecular relaxation by increasing media viscosity drastically reduce the relaxation rate and increase the radiative pathway (Loutfy & Law, 1980; Loutfy, 1981). Loutfy and Arnold (1982) have shown that, for a series of malononitrile derivatives, there is excellent agreement between the experimentally determined quantum yield and the solvent viscosity as predicted by the Förster–Hoffmann equation (1971).

We have investigated the possibility that these novel fluorescent molecules could have potential use in the direct determination of the effective microviscosities of artificial bilayers and natural membranes. The findings reported here involve the measurement of the fluorescence characteristics of 9-(dicyanovinyl)julolidine (DCVJ) in both detergent micelles (sodium dodecyl sulfate (SDS)) and DPPC vesicles. Viscosity and local dielectric properties of the probe environment in these systems are calculated and compared to values reported from other luminescent techniques.

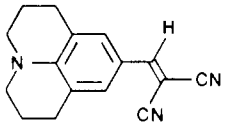

9-(dicyanovinyl)julolidine (DCVJ)

Experimental Procedures

Instrumentation. Fluorescence measurements were recorded on an SLM 4800 spectrofluorimeter coupled to a Tektronix 4051 microcomputer. The excitation wavelength was set at 430 nm. Relative fluorescence quantum yields were calculated from integrated corrected spectra with a GG21 standard block (Hellma, $\Phi_f = 0.494$) as a reference. A thermostated sample holder was used, and all temperature readings were monitored with an iron–constantan thermocouple. Absorption spectra were recorded on a Cary 210 spectrophotometer.

Materials. 9-(Dicyanovinyl)julolidine (DCVJ), prepared by the method of Kuder et al. (1977), was generously provided by Dr. R. O. Loutfy. Synthetic dipalmitoylphosphatidylcholine (DPPC) (Sigma, 99% pure) and sodium dodecyl sulfate (SDS) (99% specially pure BDH grade) were used without further purification.

Propan-2-ol (bp 82–82.4 °C) and hexan-1-ol (bp 156–157 °C) were fractionally distilled over anhydrous calcium sulfate and stored over 4-Å molecular sieves. Glycerol was obtained from Aldrich Chemical Co. (Gold Label, 99.5% spectrophotometric grade). Viscosity measurements were made at 25 °C for ethylene glycol/glycerol mixtures using Cannon-Fenske capillary tube 300 and 400 viscometers. All other solvent viscosities were obtained from literature values (Law, 1980, 1981). Other solvents were reagent grade and were used without further purification. Doubly distilled deionized water was routinely used.

Sample Preparation. Synthetic DPPC vesicles were prepared by sonicating (Braunsonic 1510 sonicator) a DPPC dispersion in 15 mM Tris-HCl (pH 7.4) buffer for 15–30 min above the phase-transition temperature (50 °C). Insoluble material was removed by centrifugation (27000*g* for 90 min).

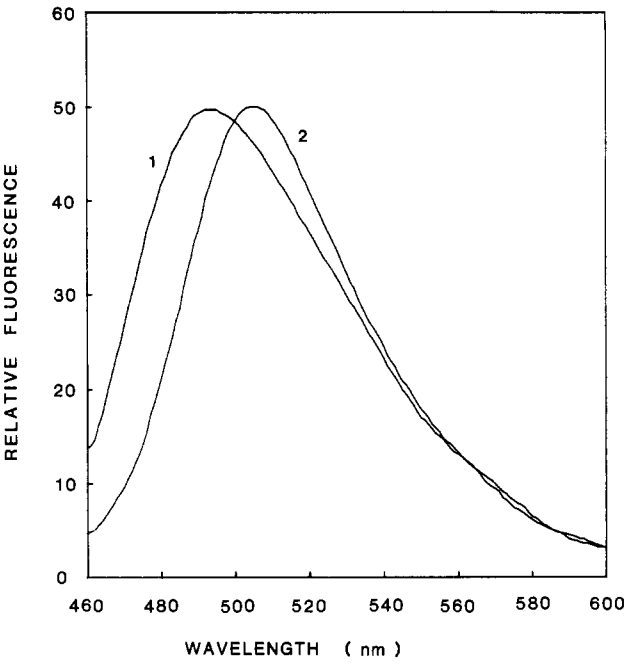

FIGURE 1: Corrected fluorescence emission spectra (arbitrary units) of 9-(dicyanovinyl)julolidine (DCVJ) in (1) ethylene glycol/glycerol (3:7, v/v) at 25 °C, λ_{max} = 505 nm, and (2) small unilamellar dipalmitoylphosphatidylcholine (DPPC) vesicles (1 mg/mL) at 33.7 °C, λ_{max} = 493 nm. The probe concentration in each solution was 4.5 μM.

Stock solutions of DCVJ were prepared in tetrahydrofuran and standardized by the molar extinction coefficient of 61.5 $\times 10^3$ M^{-1} cm^{-1}. An aliquot of probe DCVJ from a concentrated stock solution was dried under nitrogen and mixed by vortexing with a solution of DPPC vesicles (1 mg/mL) or SDS micelles (11 mM, above the critical micellar concentration). Incorporation time in vesicles was decreased by heating the solution at 47 °C for 1 h.

The final concentrations of fluorophore were normally around 4.5 μM and spectral corrections were made for scattered light where necessary.

Results

Fluorescent Properties of 9-(Dicyanovinyl)julolidine. Previous studies have shown that 9-(dicyanovinyl)julolidine (DCVJ) absorbs strongly in the blue region (≈450 nm) and has a weak green fluorescence emission (≈490 nm). As with most intramolecular charge-transfer molecules, both the absorption and emission spectra are highly solvent dependent (Loutfy & Law, 1980; Cox et al., 1984). Figure 1 shows the fluorescence spectra of DCVJ in an ethylene glycol/glycerol mixture (3:7, v/v) (λ_{max} = 505 nm) and in DPPC vesicles (λ_{max} = 493 nm). Law and Loutfy (1981) have shown that with high concentrations of similar dyes, dimers and higher aggregates form that have strong emissions around 590 nm. No such low-energy emission has been observed for DCVJ in any of the solvents, vesicles, or micelles studied. In addition, the quantum yield of DCVJ is independent of solvent polarity, which is not the case for many fluroescent molecules such as anilinonaphthalenesulfonic acid analogues commonly used as bilayer probes (Loutfy & Law, 1980; Kosower et al., 1983; Lakowicz, 1983).

In solvents of increasing dielectric constant, the fluorescence emission maximum shifts to longer wavelengths. This has been shown to result primarily from solvent stabilization of the excited intramolecular charge-transfer state (Loutfy & Law, 1980). Figure 2 shows a plot of the corrected fluorescence

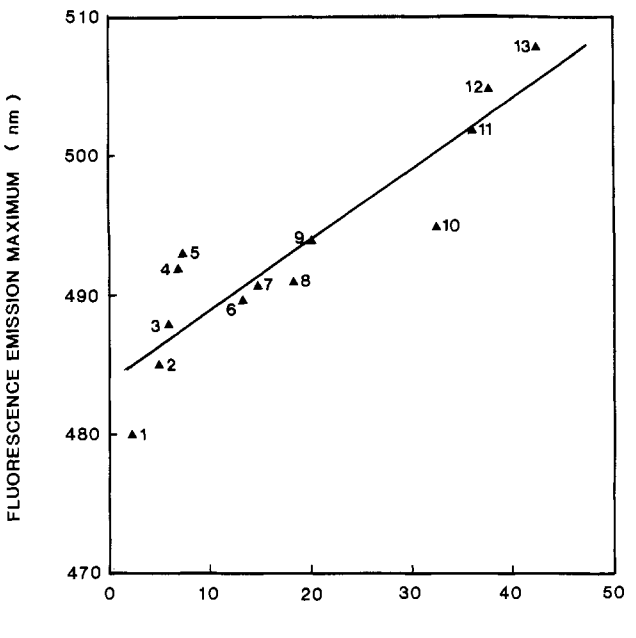

FIGURE 2: Measured fluorescence emission maxima, λ_{max} (nm), of 9-(dicyanovinyl)julolidine (DCVJ) plotted against the dielectric constants of solvents of varying polarity at 25 °C: (1) benzene; (2) *n*-butyl acetate; (3) ethyl acetate; (4) 2-methyltetrahydrofuran; (5) tetrahydrofuran; (6) 1-hexanol; (7) 3-methylbutanol; (8) 2-propanol; (9) 1-propanol; (10) methanol; (11) acetonitrile; (12) ethylene glycol; (13) glycerol. The probe concentration was 4.5 μM. The correlation coefficient is 0.911.

Table I: Dielectric Constants for Vesicles and Micelles

probe/method	system	dielectric constant	ref
9-(dicyanovinyl)julolidine	DPPC vesicles	17.9	this work
pyridinium *n*-phenolbetaine	DPPC vesicles	16–14	*b*
dipyrenylpropane (excimer)	DMPC vesicles	17.5	*c*
pyridinium *n*-phenolbetaine	DMPC vesicles	16–14	*b*
dipyrenylpropane (excimer)	EPC vesicles	17.5	*c*
9-(dicyanovinyl)juloidine	SDS micelles	41.6	this work
pyrene (diffusion excimer)	SDS micelles	45	*d*
DCQEB[a]	SDS micelles	40	*e*
dipyrenylmethyl ether (excimer)	SDS micelles	32.7	*c*
pyridinium *n*-phenolbetaine	SDS micelles	51–55	*b*

[a] 2-[6-(2,2-Dicyanovinyl)-3,4-dihydro-2,2,4-trimethyl-1(2*H*)-quinoyl]ethyl benzoate. [b] Zachariasse et al., 1981. [c] Zachariasse et al., 1982. [d] Thomas, 1980. [e] Law, 1981.

peak maxima vs. the dielectric constant for a variety of solvents. From this plot, the apparent dielectric constant for the probe in DPPC bilayers was found to be 17.9. As shown in Table I, this value agrees very well with those reported of a variety on nonpolar fluorescent molecules. In SDS micelles, the emission maximum (505 nm) corresponds to a dielectric constant of 41.6, a value considerably more polar than that for DPPC vesicles. Again, this value also agrees well with literature values (Table I).

Microviscosity Determination for DPPC Bilayers and SDS Micelles. For molecular rotors whose decay is governed by torsional relaxation, the fluorescence quantum yield has been shown to be viscosity dependent (Loutfy & Arnold, 1982). The relationship between the quantum yield of DCVJ and the solvent viscosity has been derived previously by Law (1980). The quantum yield Φ_f is related to the nonradiative rate constant k_{nr} by

$$\Phi_f = k_f/(k_f + k_{nr}) \quad (1)$$

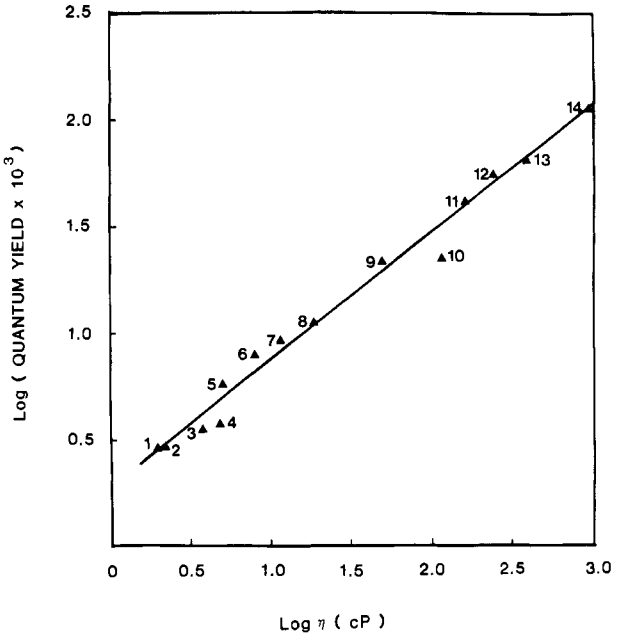

FIGURE 3: Plot of log Φ vs. log η for 9-(dicyanovinyl)julolidine (DCVJ) in solvents of varying viscosity at 25 °C in accordance with eq 5: (1) 1-propanol; (2) 2-propanol; (3) 3-methylbutanol; (4) 1-hexanol; (5) ethylene glycol/2-propanol (3:7, v/v); (6) ethylene glycol/2-propanol (5:5, v/v); (7) ethylene glycol/2-propanol (7:3, v/v); (8) ethylene glycol; (9) ethylene glycol/glycerol 7:3, v/v); (10) ethylene glycol/glycerol (5:5, v/v); (11) ethylene glycol/glycerol (4:6, v/v); (12) ethylene glycol/glycerol (3:7, v/v); (13) ethylene glycol/glycerol (2:8, v/v); (14) glycerol. The probe concentration was 4.5 μM. The correlation coefficient is 0.992.

where k_f is the intrinsic radiative rate constant. For DCVJ, k_f is 2.78×10^8 s^{-1} (Loutfy & Law, 1980). k_{nr} for this molecule is dominated by a very rapid torsional relaxation. Since $k_{nr} \approx 10^{11}$ s$^{-1} \gg k_f$, eq 1 simplifies to

$$\Phi_f = k_f/k_{nr} \quad (1a)$$

Doolittle (1952) showed that, in general, the fluid viscosity (η) is a function of the free volume (V_f) of the solvent molecule according to the equation

$$\eta = Ae^{(V_0/V_f)} \quad (2)$$

where V_0 is the van der Waals volume of the solvent molecule and A is a constant. For molecular rotors undergoing torsional relaxation, k_{nr} is controlled by the solvent free volume and can be expressed as

$$k_{nr} = k_{nr}^{\circ}e^{-x(V_0/V_f)} \quad (3)$$

where k_{nr}° is the intrinsic relaxation rate when there is no free volume dependence or when the solvent viscosity is low (Johnson, 1975; Gegiou et al., 1968). Here, x is a term that depends on the structural properties of the rotor and represents a fraction of the total critical volume for solvent motion that is required for the molecular rotor to undergo torsional rearrangement (Law, 1980). Combining eq 1a and 3

$$\Phi_f = (k_f/k_{nr}^{\circ})e^{x(V_0/V_f)} \quad (4)$$

Finally, substituting and simplifying eq 4 with 2 gives a form of the Förster–Hoffmann expression (1971):

$$\log \Phi_f = C + x(\log \eta) \quad (5)$$

where C is a constant.

The quantum yield of DCVJ was determined for solvents whose viscosities ranged from 2 cP to about 1000 cP. A plot of log Φ_f vs. log η according to eq 5 is linear as shown in Figure

Table II: Effective Microviscosities for SDS Micelles and Phospholipid Vesicles

technique (probe)	SDS micelles			phospholipid vesicles			
	T (°C)	η (cP)	ref		T (°C)	η (cP)	ref
(1) quantum yield							
9-(dicyanovinyl)julolidine	25	6.9	this work	DPPC	10–60	120–70	this work
DCQEB[a]	20	31	*c*	DPPC	10–60	30–3	*k*
DHICC[b]	20	4.3	*d*				
(2) fluorescence depolarization							
anthracene	27	17–50	*e*				
perylene	27	17–50	*e*	DPPC	25–45	940–94	*l*, *m*
perylene				EPC	25	90–130	*m*, *n*
diphenylhexatriene				DPPC	10–60	1000–50	*o*, *p*
diphenylhexatriene				EPC	25	80–97	*n*, *q*
2-methylanthracene				DPPC	20	291	*l*
(3) intramolecular excimer formation							
dipyrenylpropane	20–37	19–12	*f*, *g*	DPPC	20–50	30–18	*r*
dipyrenylpropane				DMPC	37	23	*g*
dipyrenylpropane				DMPC	10–60	125–38	*r*
diphenylpropane	20	10	*h*				
dinaphthylpropane	20–30	9–6	*i*				
di(biphenyl)methyl ether	20	10	*h*				
dipyrenylmethyl ether	37	20–50	*g*	DMPC	37	53–80	*r*
dipyrenylmethyl ether				EPC	37	69–110	*r*
(4) intermolecular excimer formation							
pyrene	25	193	*j*	DMPC	20	57.2	*s*
pyrene				EPC	30	59.2	*s*

[a] 2-[6-(2,2-Dicyanovinyl)-3,4-dihydro-2,2,4-trimethyl-1(2*H*)-quinoyl]ethyl benzoate. [b] 1,1′-Dihexyl-3,3,3′,3′-tetramethylindocarbocyanine iodide. [c] Law, 1981. [d] Greiser et al., 1985. [e] Azzi, 1975. [f] Zachariasse, 1978. [g] Zachariasse et al., 1982. [h] Emert et al., 1979. [i] Turro et al., 1979. [j] Pownall & Smith, 1973. [k] Lukac, 1984. [l] Tran et al., 1978. [m] Yguerabide & Foster, 1982. [n] Shinitzky & Barenholtz, 1974. [o] Lentz et al., 1976. [p] Lakowicz, 1983. [q] Dale et al., 1977. [r] Zachariasse et al., 1980. [s] Vanderkooi & Callis, 1974.

3. The slope of the line is $x = 0.60$, a value that agrees well with the $^2/_3$ power viscosity dependence of the quantum yield ($\Phi_f = C\eta^{2/3}$) for a number of triphenylmethane dyes reported by Förster and Hoffmann (1971). The viscosity dependence of the quantum yield from Figure 3 can now be used to calculate the effective microviscosity for DCVJ in DPPC vesicles and SDS micelles.

The effective microviscosity of SDS micelles using DCVJ is 6.9 cP, a value in the lower range of those reported using other luminescent molecules (Table II). It can be seen that the reported viscosities range from a low of 4 cP to a high of 193 cP and in some cases appear to be probe dependent. The effective microviscosity in DPPC vesicles at 25° C is 94 cP, with values ranging from 120 to 70 cP between 10 and 60 °C. Again, a comparison with literature values (Table II) reveals a large variation in microviscosity using different luminescent techniques. The possible reasons for this variance are discussed below.

Activation Energies for DPPC Hydrocarbon Chain Mobility. The temperature-dependent phase behavior of natural and artificial bilayers has been extensively studied by a number of spectroscopic and calorimetric techniques. For example, it is well-known that bilayers composed of DPPC undergo a major thermotropic change that represents a phase transition from a highly ordered gel state to a more disordered liquid-crystalline state (Houslay & Stanley, 1982).

We have monitored the change in Φ_f of DCVJ in DPPC vesicles with increasing temperature between 10 and 60 °C. All the Φ_f values fall within the range of solvents used for the standard curve shown in Figure 3. The effect of temperature on Φ_f is dominanted by the thermotropic effect of the solvent matrix on k_{nr}, and thus the fluorescence of DCVJ can be regarded as being temperature independent (Law, 1980). As a result, the variation of Φ_f in DPPC vesicles with temperature can be looked upon as an effect of temperature on the physical properties such as viscosity or hydrocarbon chain mobility of the bilayer core. A plot of the extrapolated microviscosity (η) values vs. temperature was nonlinear with a sharp decrease

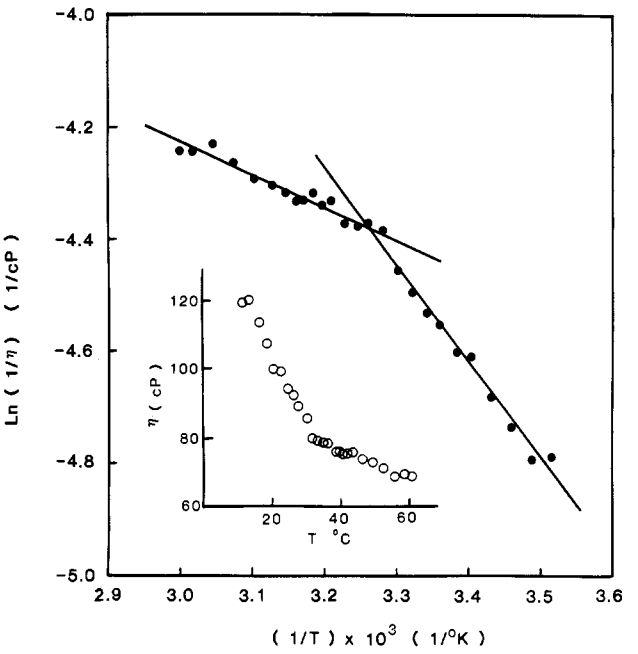

FIGURE 4: Arrhenius plot of the effect of temperature on the hydrocarbon chain mobility in DPPC vesicles according to eq 6. DPPC vesicles were 1 mg/mL, and the probe concentration was 4.5 μM. Temperature was increased from 10 to 60 °C. The correlation coefficients are 0.993 below 34 °C and 0.967 above. The inset shows the calculated effective microviscosity (η) from the standard curve shown in Figure 3 as a function of temperature.

in η below about 30 °C (Figure 4 inset). The solvent or DPPC hydrocarbon chain mobility activation energy ($\Delta E(\eta)$) can be determined from an Arrhenius-type plot of the temperature dependence of the solvent mobility ($1/\eta$) according to the equation

$$1/\eta = (1/\eta_0)e^{(-\Delta E(\eta)/kT)} \quad (6)$$

where $1/\eta_0$ is the solvent mobility in the limit as the temperature approaches infinity. The Arrhenius plot (Figure 4)

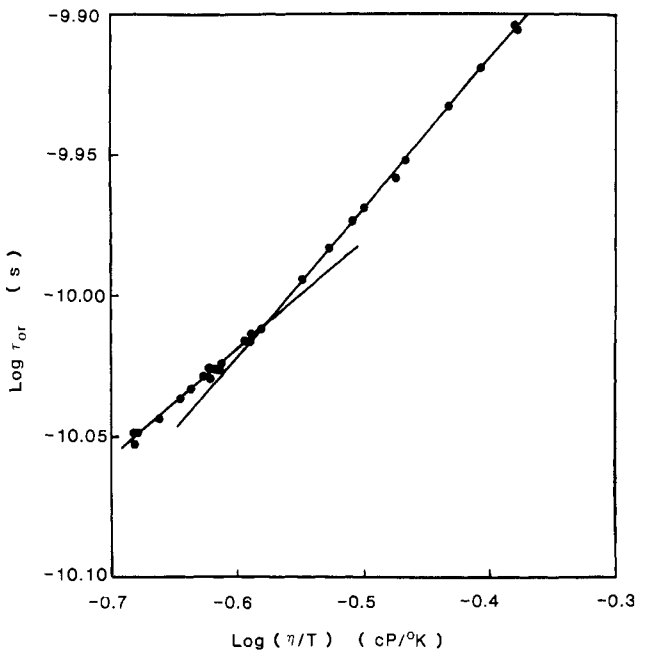

FIGURE 5: Plot of log τ_{or} vs. log (η/T) in accordance with eq 8, showing the effect of temperature and viscosity on the torsional relaxation time, τ_{or}, of DCVJ in DPPC vesicles (1 mg/mL). The correlation coefficients above and below the break (34 °C) are 0.997 and 0.999, respectively.

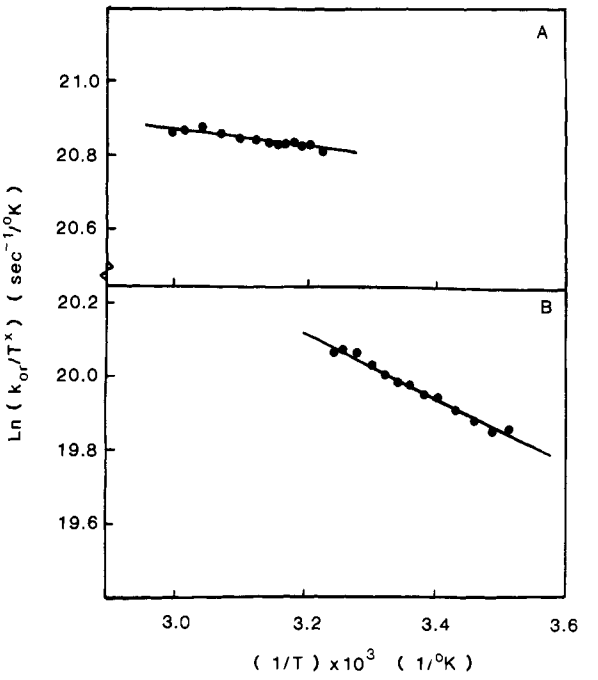

FIGURE 6: Plot of ln (k_{or}/T^x) vs. $1/T$ according to eq 9, showing the temperature dependence of the torsional relaxation rate, k_{or}, of DCVJ in DPPC vesicles (1 mg/mL) when the free volume effect is taken into consideration. The respective x values from Figure 5 were used here over two temperature ranges (x = 0.52, 10–34 °C; x = 0.39, 34–60 °C). The correlation coefficients are 0.91 and 0.99 for the high- and low-temperature regions, respectively.

for DPPC vesicles gave two straight lines with a distinct breakpoint at approximately 34 °C. From the slopes, the calculated activation energies $\Delta E(\eta)$ above and below this transition are 6.9 and 14.7 kJ/mol, respectively.

Torsional Relaxation of DCVJ in DPPC Vesicles. Where the relaxation time of the surrounding solvent matrix governs the rotational relaxation time of a molecular rotor, as is the case for the reorientation of DCVJ in the DPPC hydrocarbon matrix, k_{nr} can be approximated by the rate constant k_{or}, which is the reorientation rate constant for the probe. Therefore, k_{or} can be determined from the measured quantum yield Φ_f as

$$k_{or} \approx k_{nr} = k_f(\Phi_f^\circ - \Phi_f)/\Phi_f \qquad (7)$$

where Φ_f° is limiting quantum yield. For DCVJ, Φ_f has been shown to approach unity at 77 K and $k_f = 2.78 \times 10^8$ s^{-1} under the same conditions (Loutfy & Arnold, 1982). Loutfy and Arnold (1982) have shown that the torsional relaxation dynamics of molecular rotors in medium- to high-viscosity solvents ($\eta > 2$ cP) cannot be described by the simple stick boundary hydrodynamics defined by the Debye–Stokes–Einstein (DSE) equation ($\tau_{or} = 1/k_{or} = C(\eta/T)$). For DPPC vesicles, a plot of τ_{or} vs. (η/T) is nonlinear, and nonzero intercepts are obtained, suggesting deviation from the DSE theory (data not shown).

However, a modified form of this relationship (eq 8), which takes into account the free volume effect and thereby agrees with the Förster–Hoffmann scheme, provides a valid description of the torsional relaxation process of a series of malononitrile analogues in a variety of solvents ($\eta > 2$ cP) (Loutfy & Arnold, 1982). In (8), C is a constant and x is the free volume term as previously described. A plot of log τ_{or} vs. log (η/T) is shown in Figure 5 for DCVJ in DPPC vesicles over the temperature range 10–60 °C. Again, a visible transition occurs at approximately 34 °C. The slopes corresponding to x above and below the transition temperature are

$$\tau_{or} = C(\eta/T)^x \qquad (8)$$

0.39 and 0.52, respectively. The magnitude of these values relates to the degree to which the free volume governs k_{or} such that the smaller the value the smaller the free volume contribution. Therefore, at low temperatures where the viscosity is high and the free volume small, the free volume effect on the torsional relaxation of the dye is large. The opposite is true at high temperatures where the free volume is larger and the viscosity smaller. In low-viscosity solvents, there will be little or no dependence on the free volume (Loutfy & Arnold, 1982; Johnson, 1975).

Activation Energies for Torsional Rotor Relaxation. Since the torsional relaxation dynamics for rotor motion obeys eq 8, the relaxation rate constant of this process, k_{or}, is given by eq 9, which can be derived from eq 6 and 8. A plot of ln

$$k_{or} = (T^x/\eta_0{}^x C)e^{(-x\Delta E(\eta)/kT)} \qquad (9)$$

(k_{or}/T^x) vs. $1/T$ for DCVJ in DPPC vesicles (Figure 6) gives two slopes $[x\Delta E(\eta)/k]$ above and below the transition temperature of 34 °C. The x values used here are those obtained from Figure 5 for each respective temperature region. $\Delta E(\eta)$ in this case is equivalent to the activation energy for molecular relaxation in the solvent or $\Delta E(k_{or})$. The activation energies for torsional rotor relaxation, $\Delta E(k_{or})$, are 14.2 and 4.6 kJ/mol below and above the break point, respectively, and they closely approximate the activation energies for hydrocarbon mobility evaluated from Figure 4.

Waldeck and Fleming (1981) have shown that for the rotational relaxation of 3,3′-diethyloxadicarbocyanine iodide in a variety of low-viscosity alcohols, simple stick boundary hydrodynamic theory was indeed applicable and, in this case, eq 9 was valid for $x = 1$. The calculated activation energies, $\Delta E(\eta)$ and $\Delta E(k_{or})$, were equivalent as expected since the macroscopic solvent viscosity is a reasonable measure of the frictional drag on the molecular rotation. On the other hand, Loutfy and Arnold (1982) using the same equation showed that for medium- to high-viscosity solvents ($\eta > 2$ cP), $\Delta E(\eta)$

> $\Delta E(k_{or})$ by 12–20 kJ/mol and that simple hydrodynamics were inappropriate for this situation. A similar result was found for DPPC vesicles. Assuming $x = 1$ in eq 9, the activation energies, $\Delta E(k_{or})$, above and below the transition temperature were 0.18 and 6.7 kJ/mol, respectively, substantially less than the respective activation energies for solvent mobility, $\Delta E(\eta)$.

Discussion

Macroscopic and microscopic motions occurring within the hydrocarbon core of phospholipid bilayers may be distinguished from one another by virtue of their varying dimensional ranges. For example, macroscopic motions are mainly associated with translational or lateral diffusion of components within the bilayer (Schlessinger & Elson, 1982). Membrane viscosity values estimated from such motions may not be true "effective microviscosities" but rather a qualitative sum of viscosities representing an overall impedance of a region in the bilayer to such motions. Furthermore, the Stokes–Einstein equation, which relates the diffusion coefficient to solvent viscosity, may not be appropriate for the inhomogeneous bilayer matrix.

Microscopic motions are those restricted to molecular dimensions such as rotational diffusion. The rotational mobility of a molecule in the bilayer is a reasonable indicator for the "effective microviscosity" of the bilayer (Schlessinger & Elson, 1982). As a result, many internalized fluorophores where the fluorescence characteristics depend upon the degree of molecular rotation have been employed to measure the effective microviscosity or fluidity of the bilayer.

Steady-state depolarization techniques generally use molecules such as 1,6-diphenyl-1,3,5-hexatriene (DPH) or perylene where the fluorescence depolarization reflects molecular rotation and is therefore solvent viscosity dependent (Yguerabide & Foster, 1982; Schlessinger & Elson, 1982). However, the correlation between the motion of the molecule in pure solvents to that in anisotropic matrices such as lipid bilayers often cannot be made directly. When isotropic motion is assumed, large and possibly erroneous microviscosities are obtained. Because the probe moves anisotropically in the bilayer, constraints must be imposed on the rotational mobility of the molecule, and in conjunction, the decay of the molecule must be described multiexponentially. This has led to the development of the "wobbling in a cone" model for DPH from time-dependent fluorescence anisotropy measurements (Kawato et al., 1977; Kinosita et al., 1981). Effective microviscosities calculated by this method are smaller by 1 order of magnitude from those obtained from steady-state depolarization methods but again may be dependent upon the accurate resolution of the uneven distribution of fluorescence lifetimes.

Other luminescent methods used to determine membrane microviscosities include the measurement of intramolecular and intermolecular excimers (Zachariasse et al., 1978; Viriot et al., 1983). Since the formation of excimers is solvent viscosity and molecular structure dependent, the microviscosities reported often vary with the structural nature of the fluorophore and on the standard solvent system used for calibrating the viscosity dependence of excimer formation. In essence, these fluorophores do not exhibit rotational diffusion but rather a cooperative diffusion of neighboring chromophores. For pyrene analogues, the measured ratio of monomer to excimer intensities that is required for microviscosity calculations may also be solvent polarity dependent and thus complicate the estimation of absolute local viscosity (Zachariasse et al., 1978).

Loutfy and his colleagues (Law & Loutfy, 1981, 1983; Loutfy, 1981) have successfully used a series of [*p*-(dialkylamino)benzylidene]malononitrile analogues as probes for studying viscosity changes that occur in polymeric reaction mixtures. In these molecules, the nonradiative decay mechanism of the charge-transfer excited state is dominated by the rapid internal conversion through the torsional relaxation about the donor–acceptor bond. Restrictions to this motion brought about by increasing solvent viscosity cause a significant increase in the relative contribution to the radiative pathway for deexcitation at the expense of the nonradiative pathway (Loutfy & Law, 1980). The quantum yield of these molecules has been shown to be independent of changes in the local polarity of the environment. Furthermore, the dependence of the quantum yield on the temperature is dominated by the temperature effect on solvent viscosity (Law, 1980). Therefore, the measured quantum yield in a variety of solvents solely monitors the variations in the effective viscosity.

In medium- to high-viscosity solvents (2–1000 cP) as those shown in Figure 3, the rotational diffusion of the solvent molecules governs the amount of free volume present within the solvent. Here, the rate of solvent rotational diffusion governs the torsional rotor relaxation and therefore becomes the rate-determining step in the nonradiative deexcitation of the excited state.

The solvent viscosity dependence of the quantum yield in Figure 3 has been used to calculate the effective microviscosities of DCVJ in SDS micelles and DPPC vesicles over a broad temperature range. Implicit in this is the crucial assumption that the probe environment, namely the hydrocarbon chain region, has similar characteristics to either medium- or high-viscosity solvents. In SDS micelles at 25 °C, the effective microviscosity was found to be 6.9 cP, which compares closely with the value (4.3 cP) obtained by Greiser et al. (1985) for the molecular rotation of a carbocyanine dye, but considerably smaller than values reported using other fluorescent techniques (Table II).

In DPPC vesicles, increasing the temperature from 10 to 60 °C decreases the calculated effective microviscosities from 120 to 70 cP. In contrast, effective microviscosity values between 30 and 3 cP from 10 to 60 °C were determined by Lukac (1984), using a phenyl-substituted malononitrile analogue. We have found, in agreement with polymer studies reported by Loutfy and Law (1981), that this particular probe used by Lukac may be unsuited for bilayer viscosity studies because it readily forms dimers and higher aggregates in medium- to high-viscosity environments. This behavior, which occurs at low (μM) probe concentrations, may result from interaction between the aromatic side chain and the parent ring system.

When our microviscosity data are plotted as in Figure 4 to obtain the activation energies, $\Delta E(\eta)$, for hydrocarbon chain rotational mobility, a break point occurs at about 34 °C. This transition is lower than the midpoint (36 °C) of the main thermal-phase transition, which normally ranges between 29 and 41 °C for small unilamellar DPPC vesicles (Lentz et al., 1976).

In multilamellar DPPC dispersions, the main phase transition has been reported to occur at 41 °C along with the pretransition at 34 °C (Parente & Lentz, 1984). The broad phase transition centered at 36 °C for small unilamellar DPPC vesicles appears to result from the constrained packing of the bilayer that does not allow a significant amount of interbilayer interaction, which is a major requirement for the formation of the pretransition state in dispersions (Stamatoff et al., 1982). The breakpoint at 34 °C detected by DCVJ in small unilamellar vesicles is sharp and contrasts the broad phase transition detected by steady-state polarization and differential scanning

calorimetry (Lentz et al., 1976). It is possible that the rotating malononitrile group of DCVJ sees only a change reflected by a lateral expansion of the bilayer. This would be manifested by a sudden increase in the free volume and a corresponding decrease in microviscosity.

The activation energies, $\Delta E(\eta)$, above and below the phase transition are much smaller than the literature values (30 and 55 kJ/mol, respectively) reported for other fluorescent molecules (Zachariasse et al., 1980; Lukac, 1982; Lentz et al., 1976). In fact, the activation energy for solvent or hydrocarbon chain mobility, $\Delta E(\eta)$, is 14.6 kJ/mol for the low-temperature region. This correlates closely with the activation energies for hydrocarbon chain trans–gauche rotational isomerization. From ^{1}H NMR T_1 (spin–lattice relaxation time) studies on DMPC vesicles for the temperature range 26–41 °C, the activation energies for acyl chain trans–gauche isomerization are 6–11 kJ/mol for carbon positions 4–12 (Wu et al., 1985). ^{2}H NMR measurements on the same system report 14.6 kJ/mol for all these carbon positions (Brown & Seelig, 1979). From the estimated dielectric constant of DCVJ in DPPC vesicles, the microenvironment of the probe would correspond to a nonpolar region probably well within the bilayer core.

The low activation energies reported here for DCVJ compared to literature values from other luminescent probes suggest that the probe is able to rotate in synchrony with the localized trans–gauche isomerization associated with the hydrocarbon chains. The larger julolidine moiety of DCVJ may be expected to be stationary with respect to the fast-moving malononitrile group. Because of the small size of the rotating malononitrile group, one would expect very little, if any, perturbation of the natural hydrocarbon chain motion or packing in this region. As a result, in contrast to the motions of the larger, more bulky luminescent probes such as perylene or pyrene that require disruption of interchain packing to accommodate them, DCVJ may orient itself in such a way that the malonitrile group interacts only with the immediate hydrocarbon solvation shell.

The calculations of the effective microviscosities in DPPC vesicles assume that the hydrocarbon solvent behaves as a medium- to high-viscosity solvent. That this assumption is indeed valid is shown below. When the orientation relaxation rate, k_{or}, is free volume dependent, then eq 8 is valid and the values of x show the degree to which the free volume effect contributes to the hydrocarbon solvent viscosity. From Figure 5, there are two distinct slopes or regions corresponding to differing free volume effects within DPPC vesicles. The larger slope in the low-temperature region ($x = 0.52$) means that the free volume effect is larger over this temperature range than at the temperatures above the transition ($x = 0.39$). Loutfy and Arnold (1982) have shown for similar malononitrile analogues that $\tau_{or} \propto (\eta/T)$ for low-viscosity solvents such as ethyl acetate ($\eta = 0.44$ cP) but $\tau_{or} \propto (\eta/T)^x$ where $x = 0.5$ for dimethyl phthalate ($\eta = 14$ cP). The free volume effect present in this solvent is similar to that observed in the DPPC bilayers at least over the lower temperature range. The large effective microviscosity observed in DPPC bilayers may be a direct result of the small free volume created by the relatively slow rotational diffusion of the hydrocarbon chains.

In long-chain alcohols such as undecanol and dodecanol, the quantum yield of similar malononitrile analogues is reported to be lower than expected from values experimentally determined from their bulk or macroscopic viscosities (Law, 1980). It has been suggested that this anomalous behavior results from an unusually high free volume that exists in these solvents due to hydrocarbon chain entanglement or coiling. Therefore, the probe perceives a "low-viscosity" environment. In DPPC bilayer, the hydrocarbon chains are ordered and presumably form a closely packed solvent matrix. Thus, the change in the free volume effect at the transition temperature may result from a change in the ordering or packing of the hydrocarbon matrix.

When the solvent viscosity is medium to high ($\eta > 2$ cP), the torsional relaxation rate constant of DCVJ can be closely approximated by the rotational rate constant of the solvent as defined in eq 6 (Loutfy & Arnold, 1982). As a result, DCVJ experiences directly the rotational motion of the acyl chains in the hydrocarbon region of the lipid bilayer. The various motions of the hydrocarbon chains include axial rotations of acyl chain or the lipid molecule and the rotational trans–gauche isomerizations. ESR and NMR studies have shown that, in the bilayer, the mobility of the chain increases with the length of the chain (Houslay & Stanley, 1982). Calculation of the rotational correlation times from T_1 data yields relaxation rate constants for segments of the DPPC chain from 10^9 s^{-1} near the polar head group to 6×10^9 and 8×10^{10} s^{-1} at the penultimate methylene and terminal methyl groups, respectively (Houslay & Stanley, 1982).

The relaxation rate constant reported from NMR studies for phospholipid or acyl chain rotation is approximately 10^8 s^{-1} (Brown et al., 1983). On the other hand, the relaxation rate constant reported from ^{2}H NMR and ^{13}C NMR studies for trans–gauche isomerization of the hydrocarbon chains in DPPC bilayers varies from 3×10^{10} to 2×10^{11} s^{-1} (Brown, 1982; Brown et al., 1983; Brown & Seelig, 1979). From ^{19}F NMR data for small unilamellar DMPC vesicles, the rate constant for rotational isomerization ranges from 0.77×10^{10} to 1.35×10^{10} s^{-1} at 41 °C, for carbon positions 4–12 (Wu et al., 1985). Calculation of k_{or} values from the quantum yield of DCVJ in small unilamellar DPPC vesicles over the temperature range 34–61 °C shows that the rotational relaxation rate constant varies from 1.03×10^{10} to 1.12×10^{10} s^{-1} but changes from 8×10^9 to 1.0×10^{10} s^{-1} for temperatures 10–34 °C. Our rate constants for the torsional relaxation of DCVJ are therefore similar to those for the trans–gauche isomerization of hydrocarbon chains.

Activation energies for the rotational relaxation of DCVJ [$\Delta E(k_{or})$] are similar to the activation energies for solvent or hydrocarbon chain mobility [$\Delta E(\eta)$], assuming that the free volume concept used in determining the solvent effective microviscosity is valid. Thus, it seems reasonable to suggest that the torsional relaxation of DCVJ is directly dependent upon the reorientation dynamics of the hydrocarbon chains within the bilayer. The near equivalence of the activation energies is consistent with the view that the probe–hydrocarbon chain interactions are within the same magnitude as the localized interactions that restrict trans–gauche isomerizations.

These studies show that dyes such as DCVJ have great potential as molecular probes to monitor the dynamic and steady-state structural changes that may occur in artificial bilayers and possibly in more complex natural membranes.

ACKNOWLEDGMENTS

We are grateful to Dr. R. O. Loutfy for providing samples of the dye 9-(dicyanovinyl)julolidine used in this study and for helpful discussions.

Registry No. DCVJ, 58293-56-4; DPPC, 2644-64-6; SDS, 151-21-3.

REFERENCES

Azzi, A. (1975) *Q. Rev. Biophys. 8*, 237–316.

Brown, M. F. (1982) *J. Chem. Phys. 77*, 1576–1599.
Brown, M. F., & Seelig, J. (1979) *J. Chem. Phys. 70*, 5045–5053.
Brown, M. F., Ribeiro, A. A., & Williams, G. D. (1983) *Proc. Natl. Acad. Sci. U.S.A. 80*, 4325–4329.
Cox, G. S., Hauptman, P. J., & Turro, N. J. (1984) *Photochem. Photobiol. 39*, 597–601.
Dale, R. E., Chen, L. A., & Brand, L. (1977) *J. Biol. Chem. 252*, 7500–7510.
Doolittle, A. K. (1952) *J. Appl. Phys. 23*, 236–239.
Emert, J., Behrens, C., & Goldenburg, M. (1979) *J. Am. Chem. Soc. 101*, 771–772.
Förster, Th., & Hoffmann, G. (1971) *Z. Phys. Chem. (Weisbaden) 75*, 63–76.
Ganesh, K. N., Mitra, P., & Balasubramanian, D. (1982) *J. Phys. Chem. 86*, 4291–4293.
Gegiou, D., Muskat, K. A., & Fischer, E. (1968) *J. Am. Chem. Soc. 90*, 12–18.
Grieser, F., Lay, M., & Thitlethwaite, P. J. (1985) *J. Phys. Chem. 89*, 2065–2070.
Houslay, M. D., & Stanley, K. K. (1982) in *Dynamics of Biological Membranes: Influence on Synthesis, Structure and Function*, Wiley, New York.
Johnson, G. E. (1975) *J. Chem. Phys. 63*, 4047–4053.
Kawato, S., Kinosita, K., Jr., & Ikegami, A. (1977) *Biochemistry 16*, 2319–2324.
Kinosita, K., Jr., Kataoka, R., Kimura, Y., Gotoh, O., & Ikegami, A. (1981) *Biochemistry 20*, 4270–4277.
Kosower, E. H., Kanety, H., Dodluk, H., Striker, G., Jovin, T., Boni, H., & Huppert, D. (1983) *J. Phys. Chem. 87*, 2479–2484.
Kuder, J. E., Limburg, W. W., Pochan, J. M., & Wychick, D. (1977) *J. Chem. Soc., Perkin Trans. 2*, 1643–1651.
Lakowicz, J. R. (1983) in *Principles of Fluorescence Spectroscopy*, Plenum, New York.
Law, K. Y. (1980) *Chem. Phys. Lett. 75*, 545–549.
Law, K. Y. (1981) *Photochem. Photobiol. 33*, 799–806.
Law, K. Y., & Loutfy, R. O. (1981) *Macromolecules 14*, 587–591.
Law, K. Y., & Loutfy, R. O. (1983) *Polymer 24*, 439–442.
Lentz, B. R., Barenholtz, Y., & Thompson, T. E. (1976) *Biochemistry 15*, 4521–4528.
Loutfy, R. O. (1981) *Macromolecules 14*, 270–275.
Loutfy, R. O., & Law, K. Y. (1980) *J. Phys. Chem. 84*, 2803–2808.
Loutfy, R. O., & Arnold, B. A. (1982) *J. Phys. Chem. 86*, 4205–4211.
Lukac, S. (1982) *Photochem. Photobiol. 36*, 13–20.
Lukac, S. (1984) *J. Am. Chem. Soc. 106*, 4386–4392.
Parente, R. A., & Lentz, B. R. (1984) *Biochemistry 23*, 2353–2362.
Pownall, H. J., & Smith, L. C. (1973) *J. Am. Chem. Soc. 95*, 3136–3140.
Schlessinger, J., & Elson, E. L. (1982) in *Methods of Experimental Physics: Biophysics* (Ehrenstein, G. & Lecar, H., Eds.) Vol. 20, pp 197–225, Academic, New York.
Shinitzky, M., & Barenholtz, Y. (1974) *J. Biol. Chem. 249*, 2652–2657.
Stamatoff, J., Feuer, B., Guggenheim, H. J., Tellez, G., & Yamane, T. (1982) *Biophys. J. 38*, 217–226.
Thomas, J. K. (1980) *Chem. Rev. 80*, 283–299.
Tran, C. D., Klahn, P. L., Romero, A., & Fendler, J. H. (1978) *J. Am Chem. Soc. 100*, 1622–1626.
Turro, N. J., Aikawa, M., & Yekta, A. (1979) *J. Am. Chem. Soc. 101*, 772–774.
Vanderkooi, J. M., & Callis, J. B. (1974) *Biochemistry 13*, 4000–4006.
Viriot, M. L., Bouchy, M., Donner, M., & Andrē, J. C. (1983) *Photobiochem. Photobiophys. 5*, 293–306.
Waldeck, D. H., & Fleming, G. R. (1981) *J. Phys. Chem. 85*, 2614–2619.
Wu, W.-G., Dowd, S. R., Simplaceanu, V., Peng, Zheng-Yu, & Ho, C. (1985) *Biochemistry 24*, 7153–7161.
Yguerabide, J., & Foster, M. C. (1982) in *Molecular Biology, Biochemistry and Biophysics: Membrane Spectroscopy* (Grell, E., Ed.) Vol. 31, pp 199–269, Springer-Verlag, New York.
Zachariasse, K. A. (1978) *Chem. Phys. Lett. 57*, 429–432.
Zachariasse, K. A., Kühnle, W., & Weller, A. (1980) *Chem. Phys. Lett. 73*, 6–11.
Zachariasse, K. A., Van Phuc, N., & Kozankiewicz, B. (1981) *J. Phys. Chem. 85*, 2676–2683.
Zachariasse, K. A., Vaz, W. L. C., Sotomayor, C., & Kühnle, W. (1982) *Biochim. Biophys. Acta 688*, 323–332.